Experimental (IR, Raman) and Computational Analysis of a Series of $PtBr_2$ Derivatives: Vibrational Coupling in the Coordinated Ethylene and Pt−Br Modes

Pavel A. Dub,[†,‡] Oleg A. Filippov,[‡] Natalia V. Belkova,[‡] Mireia Rodriguez-Zubiri,[†] and Rinaldo Poli*[,†,§]

CNRS; LCC (Laboratoire de Chimie de Coordination); Université de Toulouse; UPS, INPT; 205, route de Narbonne, F-31077 Toulouse, France, A. N. Nesmeyanov Institute of Organoelement Compounds, Russian Academy of Sciences, Vavilov Street 26, 119991 Moscow, Russia, Institut Universitaire de France, 103, bd Saint-Michel, 75005 Paris, France

Received: March 17, 2009; Revised Manuscript Received: April 9, 2009

Compounds (^{n}Bu$_4$P)[PtBr$_3$(C$_2$H$_4$)] (**1**), *trans*-[PtBr$_2$(NH$_2$Ph)(C$_2$H$_4$)] (**2**), *cis*-[PtBr$_2$(NH$_2$Ph)(C$_2$H$_4$)] (**3**), (^{n}PBu$_4$)$_2$-[PtBr$_4$] (**4**), (^{n}PBu$_4$)[PtBr$_3$(NH$_2$Ph)] (**5**), and *cis*-[PtBr$_2$(NH$_2$Ph)$_2$] (**6**), as well as the trichlorido analogue of **1**, (^{n}Bu$_4$P)[PtCl$_3$(C$_2$H$_4$)] (**1^{Cl}**), have been investigated experimentally by both IR and Raman spectroscopy, and theoretically by geometry optimization and normal-mode analysis by the DFT approach. An analysis of the normal modes of coordinated ethylene in compounds **1**, **1^{Cl}**, **2**, and **3** followed by a potential energy distribution investigation shows extensive vibrational coupling between the ν(C═C) and δ_s(CH$_2$) A$_1$ modes in two bands at around 1510−1520 and 1230−1250 cm^{-1}, the latter one having greater ν(C═C) contribution. The ρ_w(CH$_2$) A$_1$ mode, the contribution of which the above two bands is negligible, is responsible for a lower-frequency band at 995−1005 cm^{-1}. A complete vibrational analysis, backed up by the DFT calculations, has also been carried out on the Pt−Br stretching vibrations of the tetrabromido complex **4**, the tribromido complexes **1** and **5**, and the dibromido complexes **2**, **3**, and **6**, and on the Pt−Cl vibrations of the analogous complex **1^{Cl}**. The study illustrates the advantages of coupling high-level computations to the vibrational analyses to make unambiguous band assignments in IR and Raman spectroscopy.

Introduction

Ethylene is a D_{2h}-symmetric planar molecule with 12 vibrational modes distributed as $3A_g(R) + A_u(\text{inactive}) + 2B_{1g}(R) + B_{1u}(IR) + B_{2g}(R) + 2B_{2u}(IR) + 2B_{3u}(IR)$ (R = Raman active, IR = infrared active), the reference frame being chosen with the z axis perpendicular to the molecular plane.[1] These modes can be separated into five stretching modes for the C═C and the four C−H bonds ($2A_g + B_{1g} + B_{2u} + B_{3u}$), four in-plane bending modes involving the HCH and CCH angles ($A_g + B_{1g} + B_{2u} + B_{3u}$), and three out-of-plane bending modes (wagging, $A_u + B_{1u} + B_{2g}$). These modes, available in many textbooks, are also given in the Supporting Information for convenience. Two Raman-active[2] modes at 1623 and 1342 cm^{-1} are usually attributed[3−10] to the A$_g$-type C═C stretching vibration $\nu_{C=C}$ and the in-plane CH$_2$-scissoring deformation (δ_s(CH$_2$)), respectively. However, vibrational coupling is expected between fundamental molecular motions that are bases of the same irreducible representation and close in frequency, thus the two above-mentioned A$_g$-type modes (labeled q$_1$ and q$_2$) include both $\nu_{C=C}$ and in-plane bending motions with different contributions as highlighted in Scheme 1. In the higher-frequency band, the C═C bond stretches while the HCH angles widen (and the CCH angles narrow), whereas the opposite combination (HCH angle narrowing and CCH angle widening together with C═C bond stretching) is observed in the lower-frequency band.[11] On the basis of an inelastic neutron scattering analysis, the contribution of $\nu_{C=C}$ in each of these bands was quantified in terms of the potential energy distribution (PED): 69 and 46 in the high- and low-frequency bands, respectively.[12] A high-level normal coordinate analysis (NCA) yields a PED of 69% $\nu_{C=C}$, 14% δ(CCH), and 17% δ(HCH) for the band at 1609 cm^{-1} and 33% $\nu_{C=C}$, 30% δ(CCH), and 37% δ(HCH) for the band at 1332 cm^{-1}.[13] Similar values have been reported by another group.[14] The A$_g$-type C−H stretching combination, which mainly contributes to a higher-frequency band (3022 cm^{-1}),[9] does not significantly contribute to these two bands.

SCHEME 1: Three Vibrational Frequencies and Normal Mode Assignments for Ethylene

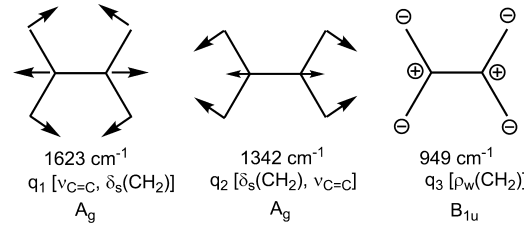

An IR-active band observed at 949 cm^{-1} is attributed to the B$_{1u}$-type out-of-plane wagging mode (ρ_w(CH$_2$)). This normal mode (labeled as q$_3$) is the only B$_{1u}$-type mode in D_{2h} symmetry and is consequently not involved in vibrational coupling. Coordination of ethylene to a metal center, however, reduces the symmetry from D_{2h} to C_{2v} at the most (if the metal complex has two perpendicular mirror planes, as for instance in Zeise's salt). Thus, all three basic molecular motions (from now on simply abbreviated as ν, δ, and ρ) become of A$_1$-type and may mix with each other in all of the above-described normal modes, the amount of mixing correlating in principle with the local

* To whom correspondence should be addressed. Fax: (+) 33-561553003. E-mail: rinaldo.poli@lcc-toulouse.fr.
† Université de Toulouse.
‡ Russian Academy of Sciences.
§ Institut Universitaire de France.

10.1021/jp902394j CCC: $40.75
Published on Web 05/08/2009

symmetry perturbation, namely with the extent of deviation from planarity. In addition to an anticipated red shift for the modes with strong ν components (q_1 and q_2), the symmetry reduction upon coordination opens the possibility of observing these modes by infrared spectroscopy ($A_g(R) \rightarrow A_1(R, IR)$).

Two models were initially proposed for coordinated ethylene and subsequently used in normal coordinate analyses: the first one based on the widely accepted[15] Chatt-Duncanson approach[16,17] whereby the ethylene H atoms move significantly away from the C_2H_4 plane; the second one, introduced by Bokii and Kukina, based on a perfectly planar arrangement for the coordinated ethylene.[18] For a variety of Pt ethylene complexes (including Zeise's salt), the band observed at 1500−1520 cm^{-1} was assigned to ν, leading Chatt and Duncanson to conclude about the "conservation of the double bond character" upon olefin coordination.[16,17] This assignment has been adopted in a few subsequent reports.[19–21] Conversely, the same band was attributed by other authors[22] to δ on the basis of comparisons with experimental and computational studies on (deutero) cyclopropane[23] and ethylene oxide.[24]

Later, two NCA on Zeise's salt were based on the Bokii-Kukina model.[25,26] In the first one, the experimentally observed band at 1526 cm^{-1} (calcd value 1528 cm^{-1}) was assigned to the A_g-type q_1 combination,[25] whereas in the second one the observed band at 1518 cm^{-1} (calcd value 1644 cm^{-1}) was interpreted as a pure ν vibration.[26] In contrast with these reports, however, another NCA using the Urey−Bradley force field assigned ν, "probably coupled with δ", to a band observed at 1243 cm^{-1}.[27] Numerous other vibrational studies of coordinated ethylene (to Pt or other metals) appeared later, occasionally without mention of vibrational coupling, with the assignment of ν to either the 1500 or the 1200 cm^{-1} band.[28]

In more recent work, the notion that ν and δ are coupled in two different normal modes q_1 and q_2 has become better appreciated. On the basis of new experimental measurements on Zeise's salt, Powell et al. concluded that ν contributes to both experimentally observed bands at ca. 1515 cm^{-1} and ca. 1240 cm^{-1} and suggested that the lower-frequency one (q_2) includes a greater proportion of ν relative to δ.[29] This assumption was later confirmed by the already mentioned inelastic neutron scattering study,[12] which reported PEDs for ν and δ in Zeise's salt of 47 and 61 in the 1515 cm^{-1} band and 50 and 30 in the 1240 cm^{-1} band, and also by a theoretical study.[13] Note that the relative contribution of ν changes on going from free ethylene (major contribution in the higher-frequency band) to coordinated ethylene (major contribution in the lower-frequency band).

However, the issue was not yet settled because until then the contribution from ρ had been neglected. A new PED analysis of Zeise's salt using a larger data set yielded decompositions into 60 (δ) + 20 (ν) + 20 (ρ) for the absorption at 1515 cm^{-1} and 60 (ν) + 25 (δ) (with no significant contribution from ρ) for that at 1240 cm^{-1}.[30] A later publication proposed that two sets of three bands (either at 1517, 1241, and 1023 cm^{-1}; or at 1517, 1410, and 1241 cm^{-1}) can be assigned to the strongly coupled ν, δ, and ρ modes.[31] However, it was concluded that "at this stage we are not able to decide which assignment is more realistic", although the second set was shown to give better agreement for complex $Pt(C_2H_4)_3$.

In more recent years, additional publications have appeared in the literature where either one or two (but not three) bands were used to describe the C═C stretching vibration. For example, in a 1995 IR study of ethylene adsorption on Pt/Al_2O_3, *only one* band at 1205 cm^{-1} was chosen to represent ν (vibrationally coupled with δ).[32] In another study limited to the 1515 and 1241 cm^{-1} bands,[33] it was pointed out that the strength of the ethylene−metal interaction determines which motion is dominant in each normal mode and that there is a crossover in relative importance. In a SERS (surface-enhanced Raman spectroscopy) study of ethylene on Pt electrodes, the observed bands at 1495 and 1210 cm^{-1} were *confidently* contributed to vibrationally coupled ν (+δ) and δ (+ν).[34] However, the authors state that "usual assignment of the higher- and lower-frequency bands to ν and δ respectively is largely formal and is sometimes reversed".[35] Finally, in two very recent contributions on Zeise's salt[36] and its tris-C_6F_5 analogue,[37] the authors reported three bands as having contributions from ν but with no mention of the ρ mode. In the first of these contributions − a variable pressure study − the weak 1515 cm^{-1} mode collapsed upon application of pressure, whereas a band at 1418 cm^{-1} with a negative pressure dependence was assigned to the ν (+δ) mode and a band at 1252 cm^{-1} with a positive pressure dependence was assigned to the δ (+ν) mode.[36] In the second paper, no absorption in the IR spectrum of compound $[Pt(C_6F_5)_3(C_2H_4)]^-$ could be unambiguously assigned to ν, but B3LYP/LANL2DZ calculations predicted three bands associated with a combination of ν and δ at 1307 (symmetric), 1501 (asymmetric), and 1584 (symmetric).[37]

Therefore, in spite of several publications on vibrational studies of coordinated ethylene, there are still many controversies with the incomplete application of previously established knowledge, plus the unresolved issue of the vibrational coupling between the ν and δ modes on one side and the ρ mode on the other side. Another problem affecting the correct assignment of the vibrational modes could be related to the nature of the metal atom, with isostructural complexes possibly showing opposite trends for the different bands as was shown for example for Zeise's salt and its Pd analogue.[38]

In the course of a recent mechanistic investigation of the $PtBr_2$-catalyzed hydroamination of ethylene and higher olefins,[39–42] we have been drawn to synthesize and fully characterize a number of $Pt^{II}-C_2H_4$ compounds with different ligand sets, notably aniline, as well as other aniline complexes that do not contain ethylene.[43] A thorough investigation of these complexes by IR and Raman spectroscopy, coupled to high-level DFT calculations, with particular focus on the vibrational modes that involve the ethylene ligand, allow us to shine more light on the vibrational coupling problem of coordinated ethylene. An analysis of other vibrations in the above compounds, notably the Pt−halogen stretching modes, will also be presented. This includes a previously unrecognized vibrational coupling and a band reassignment for the Pt−Br stretching vibrations.

Experimental Part

IR spectra were recorded on a PerkinElmer Spectrum 100 FTIR spectrometer (neat/4000−600 cm^{-1}) and on a Magna 750 Nicolet FTIR spectrometer (nujol/polyethylene: 600−50 cm^{-1}) with 2 cm^{-1} resolution. Raman spectra (solid) were recorded on a LabRAM HR 800 (HORIBA Jobin Yvon) spectrometer. ^{13}C NMR investigations were carried out on a Bruker DPX300 spectrometer operating at 75.47 MHz. All complexes used in this study have been synthesized as described elsewhere.[43] Quantum chemical calculation were performed with the *Gaussian 03* suite of programs[44] using the B3LYP functional, which includes the three-parameter gradient-corrected exchange functional of Becke[45] and the correlation functional of Lee, Yang, and Parr, which includes both local and nonlocal terms.[46,47] The basis set chosen was the standard 6-31+G*, which includes both

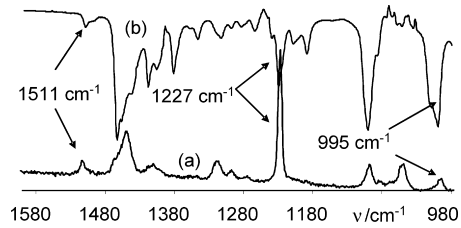

Figure 1. Raman (a) and IR (b) spectra (neat) of compound **1**.

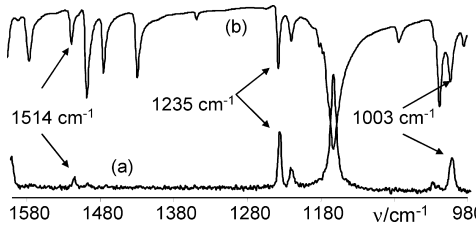

Figure 2. Raman (a) and IR (b) spectra (neat) of compound **2**.

polarization and diffuse functions that are necessary to allow angular and radial flexibility to the highly anionic systems, for all atoms of type H, C, N, and Br. The Pt atom was described by the LANL2TZ(f) basis, which is an uncontracted version of LANL2DZ and includes an f polarization function and an ECP.[48] Frequency calculations were carried out for all stationary points to verify their nature as local minima and to obtain the frequency, absorption intensity, and composition of all vibrational normal modes, under the gas-phase and harmonic approximations. The *Gaussian 03* output files where analyzed using *ChemCraft* software.[49] The normal coordinate analysis and PED calculations were performed for all gas-phase optimized complexes with the program *DISP*[50] by using equilibrium geometries and Cartesian force constants from *Gaussian* output files. *DISP* was used for transformation of the equilibrium geometries and the Cartesian force constants into the redundant internal coordinates and force constants with minimal off diagonal terms. PED was expressed as a relative contribution of each internal coordinate to the potential energy of the given normal vibration.

Results and Discussion

Compounds (^{n}Bu$_4$P)[PtBr$_3$(C$_2$H$_4$)] (**1**), *trans*-[PtBr$_2$(NH$_2$Ph)-(C$_2$H$_4$)] (**2**), *cis*-[PtBr$_2$(NH$_2$Ph)(C$_2$H$_4$)] (**3**), (^{n}PBu$_4$)$_2$[PtBr$_4$] (**4**), (^{n}PBu$_4$)[PtBr$_3$(NH$_2$Ph)] (**5**), and *cis*-[PtBr$_2$(NH$_2$Ph)$_2$] (**6**) have been investigated experimentally by both IR and Raman spectroscopy, and theoretically by geometry optimization and normal-mode analysis by the DFT approach. Compound (^{n}Bu$_4$P)[PtCl$_3$(C$_2$H$_4$)] (**1^{Cl}**) has also been investigated for comparative purposes. The theoretical study was also carried out on free C$_2$H$_4$ at the same theory level for comparison. The DFT results were subsequently used to perform potential energy distribution (PED) analyses. In the next section, we shall describe the vibrational features (with particular focus on the q_1, q_2, and q_3 vibrations) of the Pt(C$_2$H$_4$) moiety, which is present in compounds **1^{Cl}**, **1**, **2**, and **3**. Subsequently, we shall analyze the Pt−halogen modes and finally other relevant vibrations. A full list of all computed vibrational frequencies and IR intensities is provided as Supporting Information.

(a) $\nu_{C=C}$ Vibration of Coordinated Ethylene: Two or Three Bands? Experimental IR and Raman spectra in the 1600−980 cm^{-1} region for compounds **1**, **2**, and **3** are presented in Figures 1, 2, and 3, respectively. Those of compound **1^{Cl}** are available in the Supporting Information. The frequencies of the

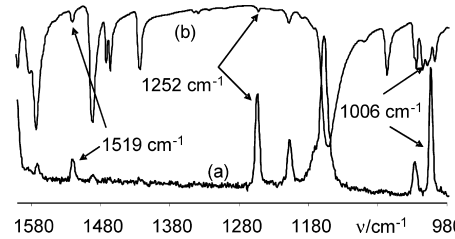

Figure 3. Raman (a) and IR (b) spectra (neat) of compound **3**.

bands that can be assigned to the three A$_1$-type normal modes q_1, q_2, and q_3 are reported in Table 1. As expected, these are located at ca. 1550, 1250, and 1000 cm^{-1}. The IR spectrum of compound (Bu$_4$N)[PtBr$_3$(C$_2$H$_4$)] has been previously reported, with a weak band at 1510 cm^{-1} in CH$_2$Cl$_2$ solution being assigned to ν.[31] Complex **2** was also previously investigated by IR spectroscopy.[51] A band observed at 1252 cm^{-1}, in perfect agreement with our data, was attributed to the ν mode without mention of vibrational coupling.

Analysis of the DFT results confirms the band assignment of Table 1. The three above-mentioned normal modes of compound **1** are shown in Figure 4. Corresponding views of those of the other three complexes are available in Figure S1 of the Supporting Information). The calculated frequencies are greater than those observed experimentally for each compound, as is usually the case for calculations done with density functional methods. However, use of an appropriate scaling factor should in principle afford a good agreement with the experimental data. Indeed, the computed frequency ratios (ν_1/ν_2 and ν_1/ν_3) are essentially identical to those obtained from the experimental data, further confirming the correctness of the band assignments. In addition, the frequencies measured for q_1 and q_2 of compound **1^{Cl}** are in good agreement with those described in several previous studies of Zeise's salt (Introduction). This also means that the nature of the cation does not affect the Pt(C$_2$H$_4$) vibration to a large extent. On the other hand, there was not universal agreement on the location of q_3. As stated in the Introduction, two sets of bands (at 1517, 1241, and 1023 cm^{-1} or at 1517, 1410, and 1241 cm^{-1}) were considered as possibilities for q_1, q_2, and q_3 in Zeise's salt, a preference being given to the latter set.[31] Our computational results, however, clearly identify the q_3 mode as the lower-frequency band (measured at 997 cm^{-1} for the PBu$_4^+$ salt).

The results of the PED analyses are also collected in Table 1. This analysis reveals that ν and δ are heavily mixed in all cases in the higher-frequency modes q_1 and q_2, and provide a small or negligible contribution to the lower-frequency q_3. Conversely, the ρ mode mostly contributes to q_3 and only to a very minor proportion to q_1 and q_2. Thus, even though the deviation from planarity of the ethylene molecule upon coordination allows mixing between ($\nu + \delta$) and ρ as discussed in the Introduction, this mixing remains in practice minimal. This is partly due to the small perturbation of the higher symmetry, and partly to the large frequency difference between the ν/δ and ρ modes, although the coordination process has the effect of raising the q_3 frequency by ca. 50 cm^{-1} and lowering the q_1 and q_2 frequencies by ca. 100 cm^{-1}, such as the ($\nu_1 - \nu_3$) and ($\nu_2 - \nu_3$) values are significantly reduced. As found in most previous studies, the major contribution of ν is found in q_2, whereas δ contributes more heavily to q_1. Thus, our analysis is fully consistent with previous results,[12,13,29] but it additionally provides a clearer picture about the location and mixing of the ρ vibration.

An analysis of the relative frequencies of q_1 and q_2 for the various compounds may provide information on the Pt−C$_2$H$_4$

TABLE 1: Observed and Calculated[a] Frequencies and PED Analysis for the q_1, q_2, and q_3 Modes of the Pt(C_2H_4) Moiety in C_2H_4 and in the Pt Complexes $\mathbf{1^{Cl}}$, 1, 2, and 3

Vibr.	C_2H_4[b]			$\mathbf{1^{Cl}}$			**1**			**2**			**3**		
	freq.		%	freq.		%	freq.		%	freq.		%	freq.		%
q_1		ν	62		ν	21		ν	22		ν	23		ν	26
	1623 R	δ_{HCH}	23	1516vw IR	δ_{HCH}	36	1510w IR	δ_{HCH}	35	1519w IR	δ_{HCH}	36	1513w IR	δ_{HCH}	34
	(1701.9)	δ_{CCH}	15	1516w R	δ_{CCH}	39	1512w R	δ_{CCH}	38	1520w R	δ_{CCH}	36	1515w R	δ_{CCH}	36
		ρ	0	(1557.1)	ρ	5	(1556.6)	ρ	4	(1576.2)	ρ	5	(1568.7)	ρ	4
q_2		ν	37		ν	76		ν	75		ν	74		ν	71
	1342 R	δ_{HCH}	39	1230m (IR)	δ_{HCH}	10	1227w IR	δ_{HCH}	11	1252w IR	δ_{HCH}	11	1236w IR	δ_{HCH}	13
	(1388.3)	δ_{CCH}	24	1230m (R)	δ_{CCH}	9	1226m R	δ_{CCH}	10	1254m R	δ_{CCH}	9	1236m R	δ_{CCH}	11
		ρ	0	(1251.3)	ρ	2	(1252.3)	ρ	1	(1283.6)	ρ	2	(1265.6)	ρ	3
q_3		ν	0		ν	0		ν	0		ν	0		ν	0
	949 IR	δ_{HCH}	0	997 (IR)	δ_{HCH}	0	995m IR	δ_{HCH}	0	1007m IR	δ_{HCH}	0	1005m IR	δ_{HCH}	0
	(974.2)	δ_{CCH}	0	997w R	δ_{CCH}	14	995w R	δ_{CCH}	90	1004m R	δ_{CCH}	14	1002m R	δ_{CCH}	12
		ρ	100	(1019.0)	ρ	90	(1016.7)	ρ	90	(1050.3)	ρ	88	(1037.1)	ρ	91
ν_1/ν_2	1.21 R (1.23)			1.23 IR 1.23 R (1.24)			1.23 IR 1.23 R (1.24)			1.21 IR 1.21 R (1.23)			1.22 IR 1.23 R (1.24)		
ν_1/ν_3	1.71 R (1.75)			1.52 IR 1.52 R (1.53)			1.52 IR 1.52 R (1.53)			1.51 IR 1.51 R (1.50)			1.51 IR 1.51 R (1.51)		

[a] IR = observed in the IR spectrum; R = observed in the Raman spectrum; the value in parentheses is that computed for the DFT-optimized geometry. [b] The Raman data for free C_2H_4 are taken from ref 1.

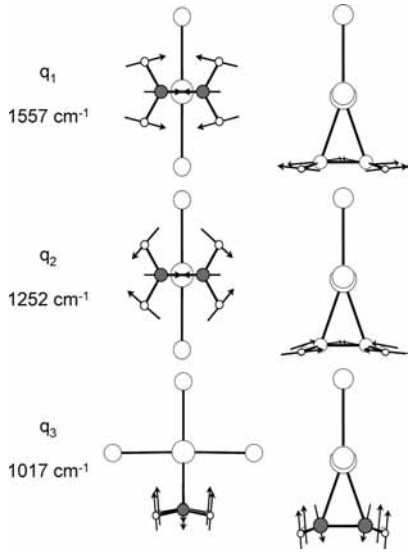

Figure 4. Two orthogonal views of the calculated normal modes q_1, q_2, and q_3 for the anion of **1**.

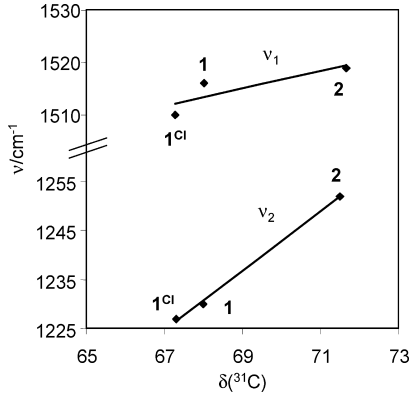

Figure 5. Correlation between the normal-mode frequencies of band 1 (a) and band 2 (b) and the olefin ligand ^{13}C NMR chemical shift for olefin complexes.

bonding. As noted above, the ν mode is more heavily contributing to q_2, for which the relative frequency trend is **2** (1252 cm^{-1}) > **3** (1236 cm^{-1}) > $\mathbf{1^{Cl}}$ (1230 cm^{-1}) > **1** (1227 cm^{-1}) for a total frequency range of 25 cm^{-1}. This trend suggests a C═C bond weakening along the same series. The mode q_1 varies to a much

TABLE 2: Experimental (IR/Raman) and Calculated Frequencies (cm^{-1}) for the $\nu(PtC_2)$ Vibrations and Optimized Pt−C and C═C Bonding Parameters (Å)[a]

	$\mathbf{1^{Cl}}$	**1**	**2**	**3**
ν_s(Pt−C_2) (A_1)	413w IR	403m IR	382w IR	386w IR
	413m R	407m R	380w R	393m R
	(408)	(393)	(371)	(377)
ν_{as}(Pt−C_2) (B_1)	507w IR	498w IR	475w IR	482m IR
	512m R	504m R	474w R	482w R
	(502)	(487)	(471)	(475)
Pt−C	2.131	2.145	2.164	2.159
	2.131	2.145	2.164	2.163
C═C	1.410	1.408	1.398	1.404

[a] IR = observed in the IR spectrum; R = observed in the Raman spectrum; the value in parentheses is that computed for the DFT optimized geometry.

smaller degree between the four compounds (10 cm^{-1} frequency range, Table 1), and the trend is not exactly the same (**2** > $\mathbf{1^{Cl}}$ > **3** > **1**), although the smaller range makes this assignment less reliable. Weakening of the C═C bond may result from either an increase of Pt → C_2H_4 π back-bonding, or an increase of Pt ← C_2H_4 σ bonding, or both. It is not possible to make conclusions about the relative effect of each of these bonding components, although both are probably contributing because there is no clear correlation with the computed Mulliken charges on the ethylene C atoms. Note that the largest frequency change for q_2 is observed on going from **2** to **3**, corresponding to a change of the ligand trans to ethylene from aniline to Br. The frequency changes are smaller when the same ligand variation occurs in the cis position or when Br is changed with Cl.

The absorption frequencies ν_1 and ν_2 are found to correlate with the $^{13}C\{^1H\}$ NMR resonance of the ethylene ligand in CD_2Cl_2 solution, as shown in Figure 5. Compound **3** could not be used for this study because it is insoluble in CH_2Cl_2. Although the validity of correlations based on only three points may be questioned, we note that analogous correlations have been highlighted between the ν_{CO} vibration of carbonyl compounds and the carbonyl ^{13}C NMR resonance.[52,53] For both bands, the compound showing the lower frequency (smaller force constant) is associated to the most upfield-shifted resonance. This appears consistent with a greater importance of π back-bonding effects. Indeed, greater π back-bonding (as expected for the anionic compounds where the charge density on the metal is greater)

TABLE 3: Calculated and Observed Frequencies and Assignments for $[PtBr_4]^{2-}$

Calcd Freq. cm^{-1}	Symmetry	Assignment, PED	Observed Frequency/cm^{-1}				
			Compd **4** (IR and R)	NBu_4^+ salt[a] (IR)	K^+ salt[b] (R)	K^+ salt[c] (IR)	K^+ salt[d] (R)
192	$1E_u$ (IR)	94% ν + 6% δ	226vs	225vs (227)		231	
176	A_{1g} (R)	ν	203s		208		214, 204[e] (208)
159	B_{1g} (R)	ν	190s		194		n.l.[f]
97	A_{2u} (IR)	ρ	110vwsh	104 ms (105)		128	
96	$2E_u$ (IR)	6% ν + 94% δ	104vw	112sh (112)		129	
93	B_{2g} (R)	δ	108m		106		189 (194)
43	B_{2u} (n.a.)[g]	ρ					

[a] From ref 56; powder data for Raman, Nujol mull data ($CHCl_3$ solution in parentheses) for IR. [b] From ref 56, H_2O solution. [c] From ref 57, single-crystal IR-reflectance (transverse optical mode, 295 K). [d] From ref 55; powder data, with solution values (D_2O) in parentheses. [e] Observed as a nonsymmetrical doublet due to a Davydov splitting. [f] Not located. [g] Not active.

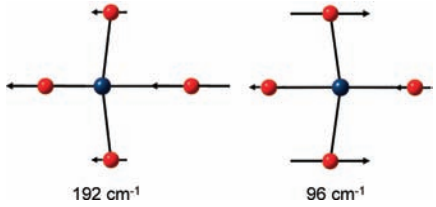

Figure 6. Calculated E_u normal modes for complex $[PtBr_4]^{2-}$ resulting from vibrational coupling between ν(Pt−Br) and δ(Br−Pt−Br).

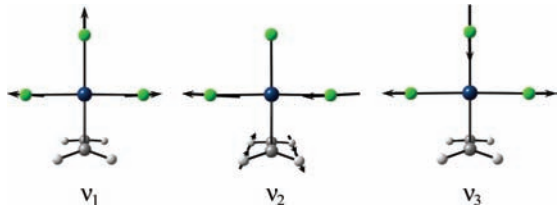

Figure 7. Normal modes of vibration for the PtX_3 moiety in compound $\mathbf{1}^{Cl}$. Compounds **1** and **5** exhibit related modes.

would not only weaken the C═C bond (lower frequency for q_1 and q_2) but also increase the electron density on the olefin ligand, inducing an upfield shift of the ^{13}C NMR resonance.

In conclusion, for all practical purposes a coordinated ethylene ligand has the ν mode distributed essentially in two normal modes, usually observed around 1500 and 1200 cm^{-1}. The contribution to the mode at ca. 1000 cm^{-1} may be neglected because it is too small. On the other hand, attributing the ν mode to only one band is incorrect because mixing between ν and δ is always extensive. At any rate, the major contribution of ν is found in the lower-frequency band at ca. 1200 cm^{-1} and not in the higher-frequency one at ca. 1500 cm^{-1}, at least for the family of Pt^{II} complexes investigated here.

The other nine normal modes of the C_2H_4 are modified only in a minor way upon coordination to the Pt atom, as shown in Table S1 of the Supporting Information. The band calculated at 1473 cm^{-1} (observed at 1406 cm^{-1}) for compound **1** and related to that previously considered as a possibility for ρ in Zeise's salt[31] is clearly originating from an asymmetric CH_2 scissoring mode (B_1), derived from $\delta(B_{3u})$ of free ethylene. Note that this band is of B_1 type in C_{2v} symmetry, thus it cannot vibrationally couple with the A_1-type q_1, q_2, and q_3 modes.

(b) ν(Pt−C) Vibrations. The symmetric and antisymmetric motions of the Pt−C_2H_4 moiety [$\nu(PtC_2)$] were assigned on the basis of the theoretical calculations and are in close agreement with those previously reported for other Pt(C_2H_4) complexes.[1,31] In all cases, the measured frequencies were higher than the calculated ones, as shown in Table 2. Both experimental and computed values are smallest for complex **2** and highest for $\mathbf{1}^{Cl}$. As expected, a stronger Pt−C_2H_4 interaction should be associated with a greater weakening of the C═C bond, thus yielding higher-frequency PtC_2 modes and lower frequencies for the q_2 mode where $\nu_{C=C}$ participates the most. Indeed, the overall trend in the two PtC_2 vibrational modes is opposite to that of ν_2 ($\mathbf{1}^{Cl} > \mathbf{1} > \mathbf{3} > \mathbf{2}$), cf. Table 2 and Table 1. As can be seen in Table 2, these trends also perfectly correlate with the optimized Pt−C and C═C distances.

(c) Pt−X Vibrations. ***(c1) Compound* 4.** The D_{4h}-symmetric square-planar $[PtBr_4]^{2-}$ complex is expected to give rise to nine vibrational modes, $A_{1\ g}(R) + B_{1g}(R) + A_{2u}(IR) + B_{2g}(R) + B_{2u}(inactive) + 2E_u(IR)$, which can be classified as four stretching modes ($A_{1g} + B_{1g} + E_u$), three in-plane bending modes ($B_{2g} + E_u$), and two out-of-plane (wagging) modes ($A_{2u} + B_{2u}$).[54] The far-IR and Raman frequencies of the $[PtBr_4]^{2-}$ complex in the PBu_4^+ salt (Figure S2 of the Supporting Information) are in good agreement with those previously reported for the $^nBu_4N^+$ and K^+ salts[55,56] (Table 3). However, some assignments made previously need to be reconsidered.

A previously unrecognized vibrational coupling in the two IR-active E_u modes is revealed by the computational results, as shown in Figure 6. The higher-frequency band calculated at 192 cm^{-1} ($1E_u$) consists mostly of ν but also has a 6% component of δ, whereas the much weaker band calculated at 96 cm^{-1} ($1E_u$) has a greater component from the bending mode and a 6% contribution from ν. The other five normal modes of the $[PtBr_4]^{2-}$ complex are shown in Figure S3 of the Supporting Information and their calculated frequencies and symmetry labels are reported in Table 3. There are three higher-frequency modes (192−159 cm^{-1}), of which only one is active in the IR, followed by a large gap with the next group of three modes in a narrow range (97−93 cm^{-1}), and a final inactive mode (B_{2u} at 43 cm^{-1}).

The $1E_u$ mode is the most easily identified mode because it is the most intense band in the IR spectrum at 226 cm^{-1} and corresponds to previously assigned bands for the K^+ and $^nBu_4N^+$ salts (Table 3).[56,57] The two other high-frequency modes (A_{1g} and B_{1g}) are visible in the Raman spectrum at 203 and 190 cm^{-1}. These assignments appear reasonable because the calculated and observed frequency ratios are quite comparable ($1E_u/A_{1g}$ calcd 1.09, found 1.11; $1E_u/B_{1g}$ calcd 1.21, found 1.19). In previous Raman studies, carried out only on the K^+ salt, the A_g mode was assigned also to a band in the same region of the spectrum at 208 cm^{-1} in aqueous solution[55,56] or to two bands at 214 and 204 cm^{-1} due to lattice effects (Davydov splitting).[55] A band around 190 cm^{-1} was also observed in the previous studies but wrongly assigned to the B_{2g} mode in one case.

For the next three bands, the assignment is more difficult given the narrow frequency range. Only one Raman active band is expected in this region and this was reported at 106 cm^{-1} for the K^+ salt in H_2O solution.[56] Compound **4** shows this band at

TABLE 4: Experimental (IR/Raman) and Calculated (Gas Phase) Frequencies (cm^{-1})[a] for the ν(Pt−X) Vibrations in Compounds 1^{Cl}, 1, and 5

	1^{Cl}			1			5		
vibr.	freq.	assign.	PED	freq.	assign.	PED	freq.	assign.	PED
ν_1(PtX) (A_1)	339vw IR[b]	ν_{ax}	58%	221m IR	ν_{ax}	86%	237vs IR	ν_{ax}	89%
	338s R	$\nu_{eq(s)}$	41%	221m R	$\nu_{eq(s)}$	10%	238vw R	$\nu_{eq(s)}$	0%
	(308.9)			(208)			(224)		
ν_2(PtX) (B_2)	333m IR	ν_{ax}	0%	241vs IR	ν_{ax}	0%	224vs IR	ν_{ax}	0%
	332vw R[b]	$\nu_{eq(as)}$	99%	242vw R	$\nu_{eq(as)}$	86%	226m R	$\nu_{eq(as)}$	95%
	(300.2)			(214)			(208)		
ν_3(PtX) (A_1)	314w IR	ν_{ax}	42%	200m IR	ν_{ax}	11%	212w IR	ν_{ax}	3%
	313w R	$\nu_{eq(s)}$	58%	201vs R	$\nu_{eq(s)}$	89%	210s R	$\nu_{eq(s)}$	85%
	(286.8)			(180)			(178)		

[a] IR = observed in the IR spectrum, R = observed in the Raman spectrum, the value in parentheses is that computed for the DFT optimized geometry. [b] Observed as a shoulder.

TABLE 5: Comparison of Pt−X Stretching Band Assignments[a]

compound	high frequency	middle frequency	low frequency	ref
Trichloride				
$K[PtCl_3(C_2H_4)]\cdot H_2O$	339 $PtCl_2$ as	331 $PtCl_2$ s	310 PtCl	25
	338 $PtCl_2$ s	327 $PtCl_2$ as	309 PtCl	27
	335 $PtCl_2$ s	328 PtCl	306 $PtCl_2$ as	56
	336 $PtCl_2$ s	330 PtCl	308 $PtCl_2$ as	56[b]
	336 $PtCl_2$ s	Not located	294 $PtCl_2$ as	36[c]
	340 $PtCl_2$ s	330 $PtCl_2$ as	305 PtCl	26
$K[PtCl_3(C_2H_4)]$	338 $PtCl_2$ s	334 PtCl	312 $PtCl_2$ as	56
$^nBu_4N[PtCl_3(C_2H_4)]$[d]	338 $PtCl_2$ s	332 PtCl	316 $PtCl_2$ as	56
$^nBu_4P[PtCl_3(C_2H_4)]$	338 PtCl (58%) + $PtCl_2$ s (41%)	332 $PtCl_2$ as	314 $PtCl_2$ s (58%) + PtCl (42%)	this work
Tribromide				
$K[PtBr_3(C_2H_4)]\cdot H_2O$	246 $PtBr_2$ as	227 $PtBr_2$ s	not located	58
$C_9H_7NH[PtBr_3(C_2H_4)]$[e]	not located	218 $PtBr_2$ as	198 PtBr	26
$^nBu_4N[PtBr_3(C_2H_4)]$	241 $PtBr_2$ as	220 PtBr	201 $PtBr_2$ s	56
$^nBu_4P[PtBr_3(C_2H_4)]$	241 $PtBr_2$ as	221 PtBr (86%) + $PtBr_2$ s (10%)	201 $PtBr_2$ s (89%) + PtBr (11%)	this work

[a] Measurements carried out in Nujol mull unless otherwise stated. [b] Measured in H_2O−HCl solution. [c] Measurement carried out under pressure. [d] Measured in $CDCl_3$ solution. [e] C_9H_7NH = quinolinium.

TABLE 6: Experimental (IR/Raman) and Calculated (Gas Phase) Frequencies (cm^{-1}) for ν(Pt−X) and δ(Pt−X) Vibrations in Compounds 2, 3, and 6

	2	3	6
$\nu_{as}(PtBr_2)$	248vs IR	222m[a](IR)[b]	222s(IR)
	249vw (R)	221m (R)[b]	222s (R)
	233 (calcd)	213 (calcd)[b]	225 (calcd)
$\nu_s(PtBr_2)$	201m (IR)	233vs (IR)[c]	228vs(IR)
	202m(R)	232vs (R)[c]	228m,sh (R)
	189,199(calcd)	237 (calcd)[c]	233(calcd)

[a] Observed as a shoulder. [b] Trans to ethylene. [c] Trans to aniline.

108 cm^{-1}. The other two bands in this group, A_{2u} and $2E_u$, are IR active. Our measured spectrum shows a band at 104 cm^{-1} with a shoulder at ca. 110 cm^{-1}, similar to the spectrum reported for the $^nBu_4N^+$ salt.[56] According to the calculation, the $2E_u$ band is more intense than the A_{2u} band (2.44 vs 1.37), thus the assignment of the 104 cm^{-1} band to the $2E_u$ mode appears more consistent.

***(c2) Trihalo Anions* 1^{Cl}, 1, *and* 5.** In these compounds, the three Pt−X (X = Cl or Br) bonds afford three stretching modes, two in-plane bending modes, and two out-of-plane bending modes, the last two being mixed with the out-of-plane Pt−C_2H_4 bending motions. The experimental IR and Raman spectra of these compounds in the low-frequency region are available in Figures S4 and S5 of the Supporting Information, respectively. Only the stretching modes, shown in Figure 7 for compound 1^{Cl} as an example, will be analyzed in detail (Table 4). The in-plane bending modes, for which only partial and tentative assignment of the spectra could be made, are shown in Figure S6 of the Supporting Information together with the experimental IR and Raman spectra (Figures S4 and S5 of the Supporting Information).

In several contributions reporting a vibrational analysis of T-shaped MX_3 moieties, the three stretching modes are described as one axial (ν_{axial}, A_1) and two equatorial (a symmetric A_1, $\nu_{eq,s}$, and an antisymmetric B_1, $\nu_{eq,as}$) modes. However, like the A_1-type $\nu_{C=C}$ and $\delta_s(CH_2)$ modes described in part *a*, vibrational coupling is to be expected and indeed the calculations yield two A_1 normal modes with contribution from all three Pt−X bonds. The higher-frequency ν_1 mode is an in-phase motion of all three Pt−X bonds, whereas in ν_3 the two mutually trans Pt−X bonds move in-phase with respect to each other and out-of-phase with respect to the axial Pt−X bond (trans to the olefin). The B_2 stretching mode (ν_2) is an out-of-phase stretching of the mutually trans Pt−X bonds, with no contribution from the axial Pt−X bond. The contribution of axial and equatorial Pt−X vibrations to each of these modes is revealed by a PED analysis, the results of which are also reported in Table 4. It is interesting to compare the Cl/Br substitution ($\mathbf{1}^{Cl}$ vs **1**) and also the C_2H_4/$PhNH_2$ substitution (**1** vs **5**). The highest-frequency stretching modes are ν_1 for $\mathbf{1}^{Cl}$ and ν_2 for **1**, according to the calculations. On going from **1** to **5** (C_2H_4/$PhNH_2$ substitution),

TABLE 7: Experimental (IR/Raman) and Calculated (Gas Phase) Frequencies (cm^{-1}) for ν(Pt−N) and ν(C−N) Vibrations in Compounds 2, 3, 5, and 6

	2		3		5		6	
ν/$cm^{-1}$$_{assnmt}$ or d_{AA}/Å	calcd	exptl	calcd	exptl	calcd	exptl	calcd	exptl
ν(Pt−N)	555	430m (IR)	557	432m (IR)	557	442m (IR)	563ν_{as}, 561ν_s	455s, 443s (IR)
	421	431m (IR)	426	431m (IR)	415	440m (IR)	442ν_{as}, 438ν_s	445m (R)
d_{PtN}	2.137		2.147		2.116		2.122	

however, ν_1 becomes again the higher-frequency mode. The ν_3 mode is the lowest-frequency stretching mode for all three complexes.

It is interesting to note that the axial and equatorial Pt−X bond stretches are heavily mixed in ν_1 and ν_3 for compound $\mathbf{1}^{Cl}$, much less so for compound **1**, and not at all for compound **5**. The new assignments backed up by our DFT calculations are compared with those previously published by other authors in Table 5. Only one of the previously published assignments for the $[PtBr_3(C_2H_4)]^-$ complex ($^nBu_4N^+$ salt[56]) is essentially in agreement with ours, except for the neglect of a small mixing of the symmetric equatorial $PtBr_2$ vibration in the middle-frequency mode and a similarly small mixing of the unique PtBr vibration in the low-frequency mode. The other two studies[26,58] report only two of the three possible bands, with assignments in disagreement with ours. Concerning Zeise's salt, many different assignments have been made, all of them attributing the higher-frequency band to either the symmetric or the asymmetric $PtCl_2$ vibration. On the other hand, there is high mixing between symmetric $PtCl_2$ and PtCl vibrations according to our calculations, and the strongest contribution to the higher-frequency band is in fact provided by the latter.

(c3) Neutral Dihalo Complexes 2, 3, and 6. The vibrational properties of compound **2** have already been reported.[51,59] However, the study was limited to IR and only one stretching vibration was reported at 248 cm^{-1}. We find (Table 6 and Figures S4 and S5 of the Supporting Information) an intense band in the IR at the same frequency (also visible as a weaker band in the Raman spectrum at 249 cm^{-1}, calculated at 223 cm^{-1}), which can be assigned to the asymmetric $PtBr_2$ vibration on the basis of the calculations. On the other hand, two bands at 199 and 189 cm^{-1} are predicted by the calculations to be associated with the symmetric $PtBr_2$ vibration because of vibrational coupling with the aniline and ethylene ligand deformations. These are seen as two intense bands at 202 and 212 cm^{-1} in the Raman spectrum, whereas they are weaker in the IR spectrum (201 cm^{-1} with a lower-intensity shoulder on the higher-frequency side). A relatively strong band observed in the IR spectrum at 195 cm^{-1} (not visible in the Raman spectrum) can be assigned to a C_2H_4−Pt−NH_2Ph bending mode (calculated at 185 cm^{-1}). A band at 195 cm^{-1} (but none at 201 cm^{-1}) was also reported in ref 59 without assignment.

Complex **3** features two Pt−Br stretching vibrations that are seen as the most intense bands in the low-frequency region both in the IR and in the Raman spectrum (Table 6). According to the calculations, the lower-frequency band has the major component from the Pt−Br bond trans to ethylene (with the longer bond of 2.482 Å), with a small in-phase component from the other bond. The higher-frequency band is an out-of-phase component with the major contribution from the Pt−Br bond trans to aniline (with the shorter bond of 2.449 Å). The small coupling between these two bonds is probably related to the electronic asymmetry of the molecule.

The vibrational properties of compound **6** have already been reported.[60] However, like in the case of compound **2**, the study was limited to IR and only one stretching vibration was reported at 223 cm^{-1}. Like complex **3**, we find complex **6** to feature two high-intensity Pt−Br stretching vibrations both in the IR and in the Raman spectrum, at frequencies very close to those of **3** (Table 6). However, contrary to **3**, the electronic symmetry in **6** favors a strong coupling and thus symmetric and asymmetric combinations are observed, each having equal contribution from the two Pt−Br bonds. Note that, for the trans arrangement in **2**, the in-phase mode ($\nu_s(PtBr_2)$) is seen at lower frequency relative to the out-of-phase mode ($\nu_{as}(PtBr_2)$), whereas the reverse is true for the cis arrangement of **6**.

(d) ν(Pt−N) Vibrations. To complete the analysis of Pt-ligand stretching vibrations, we have also examined the Pt−N stretch for all complexes containing aniline. The calculated and experimental frequencies are summarized in Table 7. For all compounds, the Pt−N stretching vibration is strongly coupled with ring vibrations and thus substantially contributes to two different vibrational modes. These are shown in the Supporting Information for the specific case of compound **5** (Figure S7 of the Supporting Information). For this reason, there is no clear correlation between either of the two frequencies and the calculated Pt−N bond length (also reported in Table 7). The previously reported vibrational analysis, limited to IR, of compound **2** attributes the Pt−N stretching vibration to a band observed[51] at 434 cm^{-1}, whereas the analysis of compound **6** attributed it to the Pt−N stretch bands at 367 and 290 cm^{-1}.[60] For each of compounds **2**, **3**, and **5**, we observe a band in the 430−450 cm^{-1} region and also two bands around 550 cm^{-1}, one of which is probably related to the combination mode with the ν(Pt−N) component. For compound **6**, two bands of similar intensity are observed at ca. 450 cm^{-1}, whereas the 550 cm^{-1} region of the spectrum is similar to that of the other compounds.

Conclusion

Our spectroscopic analysis of a few $PtBr_2$ derivatives, triggered by a theoretical study of these compounds in relation to their possible involvement in ethylene hydroamination catalysis, has led us to reconsider several band assignments made for these and related compounds in the literature, including some relatively recent contributions. The main contributions of the present study have been the recognition of previously unsuspected vibrational couplings (notably for $PtBr_n$ fragments with $n = 2$, 3, and 4) and an analysis of its limitations (notably for the q_1, q_2, and q_3 modes of coordinated C_2H_4). It has been shown that a satisfactory interpretation of the experimental spectra can be provided on the basis of high-level DFT calculations. Given the ready availability of computational tools, it is now possible to reconsider previously dubious assignments of spectral features and put vibrational analysis on a more solid basis as a characterization tool for new compounds.

Acknowledgment. We thank the CNRS and the RFBR for support through a France−Russia (RFBR−CNRS) bilateral grant No. 08-03-92506, and the MENESR (Ministère de l'Éducation nationale de l'enseignement supérieur et de la recherche de France) for a Ph.D. fellowship to P.D.

Supporting Information Available: Figures of symmetric vibrations, calculated frequencies, IR spectra, Raman spectra, tables of Cartesian coordinates for DFT-optimized geometries, and so forth. This material is available free of charge via the Internet at http://pubs.acs.org.

References and Notes

(1) Nakamoto, K. *Infrared and Raman Spectra of Inorganic and Coordination Compounds, Part B*, 5th Ed.; John Wiley & Sons Inc.: New York, 1997.

(2) Bonner, L. G. *J. Am. Chem. Soc.* **1936**, *58*, 34–39.

(3) Herzberg, G. *Molecular Spectra and Molecular Structure*; Van Nostrand: Princeton, 1945; Vol. 2.

(4) Bellamy, L. J. *The Infrared Spectra of Complex Molecules*, 3rd Ed.; Chapman and Hall: New York, 1975; Vol. 1.

(5) Socrates, G. *Infrared Characteristic Group Frequencies*, John Wiley & Sons: New York, 1980.

(6) *NIST Chemistry Webbook, http://vpl.astro.washington.edu/spectra/c2h4.htm*.

(7) Knippers, W.; Vanhelvoort, K.; Stolte, S.; Reuss, J. *Chem. Phys.* **1985**, *98*, 1–6.

(8) Piancastelli, M. N.; Kelly, M. K.; Kilday, D. G.; Margaritondo, G.; Frankel, D. J.; Lapeyre, G. J. *Phys. Rev. B: Condens. Matter Mater. Phys.* **1987**, *35*, 1461–1464.

(9) Georges, R.; Bach, M.; Herman, M. *Mol. Phys.* **1999**, *97*, 279–292.

(10) Ahern, A. M.; Garrell, R. L.; Jordan, K. D. *J. Phys. Chem.* **1988**, *92*, 6228–6232.

(11) Many spectroscopy books assign these two bands to pure $\nu_{C=C}$ and $\delta_s(CH_2)$ vibrations without mentioning the possibility of mixing. Others incorrectly report the opposite combinations of $\nu_{C=C}$ and $\delta_s(CH_2)$ (e.g., C═C bond stretching and HCH angles narrowing in the higher-frequency mode, and vice versa).

(12) Jobic, H. *J. Mol. Struct.* **1985**, *131*, 167–175.

(13) Burgina, E. B.; Yurchenko, E. N. *J. Mol. Struct.* **1984**, *116*, 17–27.

(14) Manceron, L.; Andrews, L. *J. Phys. Chem.* **1989**, *93*, 2964–2970.

(15) Love, R. A.; Koetzle, T. F.; Williams, G. J. B.; Andrews, L. C.; Bau, R. *Inorg. Chem.* **1975**, *14*, 2653–2657.

(16) Chatt, J.; Duncanson, L. A. *J. Chem. Soc.* **1953**, 2939–2947.

(17) Chatt, J.; Duncanson, L. A.; Guy, R. G. *Nature* **1959**, *184*, 526–527.

(18) Bokii, G. B.; Kukina, G. A. *Kristallografiya* **1957**, *2*, 400–407.

(19) Jonassen, H. B.; Field, J. E. *J. Am. Chem. Soc.* **1957**, *79*, 1275–1276.

(20) Powell, D. B.; Sheppard, N. *Spectrochim. Acta* **1958**, *13*, 69–74.

(21) Adams, D. M.; Chatt, J. *Chem. Ind.* **1960**, 149.

(22) Babushkin, A. A.; Gribov, L. A.; Gel'man, A. D. *Dokl. Akad. Nauk SSSR* **1958**, *123*, 461–463.

(23) Sverdlov, L. M.; Krainov, E. P. *Opt. Spektrosk.* **1957**, *3*, 54–60.

(24) Kohlrausch, K. W. F.; Reitz, A. W. *Proc. - Indian Acad. Sci., Sect. A* **1938**, *8A*, 255–266.

(25) Grogan, M. J.; Nakamoto, K. *J. Am. Chem. Soc.* **1966**, *88*, 5454–5460.

(26) Pradilla-Sorzano, J.; Fackler, J. P., Jr. *J. Mol. Spectrosc.* **1967**, *22*, 80–98.

(27) Hiraishi, J. *Spectrochim. Acta, Part A* **1969**, *25*, 749–760.

(28) Hartley, F. R. *Comprehensive Organometallic Chemistry*; Wilkinson, G., Stone, F. G. A., Abel, E. W., Eds. Pergamon Press: Elmsford, NY, 1982; Vol. 6, pp 471−762, and references therein.

(29) Powell, D. B.; Scott, J. G. V.; Sheppard, N. *Spectrochim. Acta, Part A* **1972**, *28*, 327–335.

(30) Crayston, J. A.; Davidson, G. *Spectrochim. Acta, Part A* **1987**, *43A*, 559–564.

(31) Mink, J.; Papai, I.; Gal, M.; Goggin, P. L. *Pure Appl. Chem.* **1989**, *61*, 973–978.

(32) Celio, H.; Trenary, M.; Robota, H. J. *J. Phys. Chem.* **1995**, *99*, 6024–6028.

(33) Maslowsky, E., Jr. *Vibrational Spectra of Organometallic Compounds*; Wiley: New York, 1977.

(34) Mrozek, M. F.; Weaver, M. J. *J. Phys. Chem. B* **2001**, *105*, 8931–8937.

(35) See ref 16 in ref 34.

(36) Baldwin, J. A.; Gilson, D. F. R.; Butler, I. S. *J. Organomet. Chem.* **2005**, *690*, 3165–3168.

(37) Fornies, J.; Martin, A.; Martin, L. F.; Menjon, B.; Tsipis, A. *Organometallics* **2005**, *24*, 3539–3546.

(38) Bencze, E.; Papai, I.; Mink, J.; Goggin, P. L. *J. Organomet. Chem.* **1999**, *584*, 118–121.

(39) Brunet, J. J.; Cadena, M.; Chu, N. C.; Diallo, O.; Jacob, K.; Mothes, E. *Organometallics* **2004**, *23*, 1264–1268.

(40) Brunet, J. J.; Chu, N. C.; Diallo, O. *Organometallics* **2005**, *24*, 3104–3110.

(41) Rodriguez-Zubiri, M.; Anguille, S.; Brunet, J.-J. *J. Mol. Catal. A* **2007**, *271*, 145–150.

(42) Brunet, J.-J.; Chu, N.-C.; Rodriguez-Zubiri, M. *Eur. J. Inorg. Chem.* **2007**, *471*, 1–4722.

(43) Dub, P. A. Rodriguez-Zubiri, M. Daran, J.-C. Brunet, J.-J.; Poli, R., submitted.

(44) Frisch, M. J.; Schlegel, G. W. T. H. B.; Scuseria, G. E.; Robb, M. A.; Cheeseman, J. R.; Montgomery, J.; Vreven, J. A. T.; Kudin, K. N.; Burant, J. C.; Millam, J. M; Iyengar, S. S.; Tomasi, J.; Barone, V.; Mennucci, B.; Cossi, M. ; Scalmani, G.; Rega, N.; Petersson, G. A; Nakatsuji, H.; Hada, M.; Ehara, E.; Toyota, K.; Fukuda, R.; Hasegawa, J.; Ishida, M.; Nakajima, T.; Honda, Y.; Kitao, O.; Nakai, H.; Klene, M. X.; Li, X.; Knox, J. E.; Hratchian, H. P.; Cross, J. B.; Adamo, C.; Jaramillo, J.; Gomperts, R.; Stratmann, R. E.; Yazyev, O.; Austin, A. J.; Cammi, R.; Pomelli, J. W.; Ochterski, J. W.; Ayala, P. Y.; Morokuma, K.; Voth, G. A.; Salvador, P.; Dannenberg, J. J.; Zakrzewski, V. G.; Dapprich, S.; Daniels, A. D.; Strain, M. C.; Farkas, O.; Malick, D. K.; Rabuck, A. D.; Raghavachari, K.; Foresman, J. B.; Ortiz, J. V.; Cui, Q.; Baboul, A. G.; Clifford, S.; Cioslowski, J.; Stefanov, B. B.; Liu, G.; Liashenko, A.; Piskorz, P.; Komaromi, I.; Martin, R. L.; Fox, D. J.; Keith, T.; Al-Laham, M. A.; Peng, C. Y.; Nanayakkara, A.; Challacombe, M.; Gill, P. M. W.; Johnson, B.; Chen, W.; Wong, M. W.; Gonzalez, C.; Pople, J. A. *Gaussian 03*, Rev. C.02; Gaussian, Inc.: Wallingford, CT, 2004.

(45) Becke, A. D. *J. Chem. Phys.* **1993**, *98*, 5648–5652.

(46) Lee, C. T.; Yang, W. T.; Parr, R. G. *Phys. Rev. B* **1988**, *37*, 785–789.

(47) Miehlich, B.; Savin, A.; Stoll, H.; Preuss, H. *Chem. Phys. Lett.* **1989**, *157*, 200–206.

(48) Roy, L. E.; Hay, P. J.; Martin, R. L. *J. Chem. Theory Comput.* **2008**, *4*, 1029–1031.

(49) Zhurko, G. A. *ChemCraft*, Version 1.5 (Build 245); http://www.chemcraftprog.com/, 2007.

(50) Yagola, A. G.; Kochikov, I. V.; Kuramshina, G. M.; Pentin, Y. A. *InVerse Problems of Vibrational Spectroscopy*; VSP: Utrecht, 1999.

(51) Foulds, G. A.; Hall, P. S.; Thornton, D. A. *J. Mol. Struct.* **1984**, *117*, 95–101.

(52) Legrand, N.; Bondon, A.; Simonneaux, G.; Jung, C.; Gill, E. *FEBS Lett.* **1995**, *364*, 152–156.

(53) Potter, W. T.; Hazzard, J. H.; Choc, M. G.; Tucker, M. P.; Caughey, W. S. *Biochemistry* **1990**, *29*, 6283–6295.

(54) See ref 1, Part AP 204−208.

(55) Degen, I. A.; Rowlands, A. J. *Spectrochim. Acta, Part A* **1991**, *47*, 1263–1268.

(56) Goggin, P. L.; Mink, J. *J. Chem. Soc., Dalton Trans.* **1974**, 1479–1483.

(57) Adams, D. M.; Hills, D. J. *J. Chem. Soc., Dalton Trans.* **1977**, 947–948.

(58) Foulds, G. A.; Hall, P. S.; Thornton, D. A.; Watkins, G. M. *Spectrochim. Acta, Part A* **1992**, *48*, 597–604.

(59) Heyde, T.; Foulds, G. A.; Thornton, D. A.; Desseyn, H. O.; Vanderveken, B. J. *J. Mol. Struct.* **1983**, *98*, 11–18.

(60) Auf der Heyde, T. P. E.; Foulds, G. A.; Thornton, D. A.; Watkins, G. M. *J. Mol. Struct.* **1981**, *77*, 19–24.

JP902394J